Neuropharmacology xxx (2015) 1–14

Contents lists available at ScienceDirect

Neuropharmacology

journal homepage: www.elsevier.com/locate/neuropharm

Contrasting gene expression patterns induced by levodopa and pramipexole treatments in the rat model of Parkinson's disease

Irene R. Taravini [a, *, 1], Celia Larramendy [a, 1], Gimena Gomez [a], Mariano D. Saborido [a], Floor Spaans [b], Cristóbal Fresno [c], Germán A. González [c], Elmer Fernández [c], Mario G. Murer [d], Oscar S. Gershanik [a]

[a] Laboratorio de Parkinson Experimental, Instituto de Investigaciones Farmacológicas (ININFA-CONICET-UBA), Ciudad Autónoma de Buenos Aires, Argentina
[b] Division of Medical Biology, Department of Pathology and Medical Biology, University Medical Center Groningen, University of Groningen, Groningen, The Netherlands
[c] Facultad de Ingeniería, Universidad Católica de Córdoba, CONICET, Córdoba, Argentina
[d] Laboratorio de Fisiología de Circuitos Neuronales, Instituto de Fisiología y Biofísica (IFIBIO Houssay), CONICET. Facultad de Medicina, Universidad de Buenos Aires, Ciudad Autónoma de Buenos Aires, Argentina

ARTICLE INFO

Article history:
Received 7 February 2015
Received in revised form
9 April 2015
Accepted 13 April 2015
Available online xxx

Keywords:
Parkinson's disease
Levodopa
Pramipexole
Transcriptome
Striatum
Differential transcript expression patterns

ABSTRACT

Whether the treatment of Parkinson's disease has to be initiated with levodopa or a D2 agonist like pramipexole remains debatable. Levodopa is more potent against symptoms than D2 agonists, but D2 agonists are less prone to induce motor complications and may have neuroprotective effects. Although regulation of plastic changes in striatal circuits may be the key to their different therapeutic potential, the gene expression patterns induced by *de novo* treatments with levodopa or D2 agonists are currently unknown. By studying the whole striatal transcriptome in a rodent model of early stage Parkinson's disease, we have identified the gene expression patterns underlying therapeutically comparable chronic treatments with levodopa or pramipexole. Despite the overall relatively small size of mRNA expression changes at the level of individual transcripts, our data show a robust and complete segregation of the transcript expression patterns induced by both treatments. Moreover, transcripts related to oxidative metabolism and mitochondrial function were enriched in levodopa-treated compared to vehicle-treated and pramipexole-treated animals, whereas transcripts related to olfactory transduction pathways were enriched in both treatment groups compared to vehicle-treated animals. Thus, our data reveal the plasticity of genetic striatal networks possibly contributing to the therapeutic effects of the most common initial treatments for Parkinson's disease, suggesting a role for oxidative stress in the long term complications induced by levodopa and identifying previously overlooked signaling cascades as potentially new therapeutic targets.

Abbreviations: 6-OHDA, 6-hydroxydopamine; DA, dopamine; Gabarap, Gamma-aminobutyric acid receptor-associated protein; GAPDH, Glyceraldehyde 3-phosphate dehydrogenase; GFAP, glial fibrillary acidic protein; GPx, glutathione peroxidase; HPRT, Hypoxanthine-guanine phosphoribosyltransferase; KEGG, Kyoto Encyclopedia of Genes and Genomes; LES-LEVO, group of lesioned rats treated with levodopa; LES-PRAMI, group of lesioned rats treated with pramipexole; LES-VEH, group of lesioned rats treated with vehicle; Mybl1, myeloblastosis oncogene-like 1; Ndufa12, NADH dehydrogenase (ubiquinone) 1 alpha subcomplex, 12; NORM-VEH, group of normal rats treated with vehicle; Nr4a2, Nurr1, nuclear receptor subfamily 4, group A, member 2; Olr1375, olfactory receptor 1375; PBS, phosphate-buffered saline; PD, Parkinson's disease; Ppp1r2, Protein phosphatase inhibitor 2; Psmd14, proteasome (prosome, macropain) 26S subunit, non-ATPase, 14; qRT-PCR, quantitative real-time RT-PCR; SHAM, rats injected with vehicle instead of 6-OHDA; SNpc, substantia nigra pars compacta; Sod1, superoxide dismutase 1; TH, tyrosine hydroxylase; TH-ir, TH-immunoreactive.

* Corresponding author. Laboratorio de Parkinson Experimental, Instituto de Investigaciones Farmacológicas, Facultad de Farmacia y Bioquímica. Junín 956 5° piso, (C1113AAD), Ciudad Autónoma de Buenos Aires, Argentina. Tel.: +54 11 4961 5949; fax: +54 11 4963 8593.
E-mail addresses: taravini@ffyb.uba.ar (I.R. Taravini), celialarramendy@gmail.com (C. Larramendy), gimenagomez@gmail.com (G. Gomez), marianosaborido@gmail.com (M.D. Saborido), f.spaans@umcg.nl (F. Spaans), cfresno@bdmg.com.ar (C. Fresno), ggonzalez@bdmg.com.ar (G.A. González), efernandez@bdmg.com.ar (E. Fernández), gmurer@gmail.com (M.G. Murer), gersha@gmail.com (O.S. Gershanik).
[1] Co-first authors, contributed equally.

http://dx.doi.org/10.1016/j.neuropharm.2015.04.018
0028-3908/

1. Introduction

Levodopa and pramipexole are two of the most frequently used agents for the symptomatic treatment of Parkinson's disease (PD). These two drugs differ significantly in terms of their pharmacokinetic and pharmacodynamic profiles. Levodopa is a pro-drug that needs to be enzymatically converted into dopamine (DA) within the brain to be able to stimulate all DA receptors (Cotzias et al., 1969). Pramipexole acts directly on DA receptors of the D2 family with special affinity for D3 receptors (Bennett and Piercey, 1999). Their half-lives are quite different; pramipexole has a half-life of more than six hours, while levodopa has a very short half-life of less than two hours. These differences account in part for their clinical effects. Levodopa is the most potent in terms of symptomatic improvement, but its short half-life and its effects on both DA receptors subfamilies (D1 and D2) are believed to be responsible for the development of troublesome motor complications after long-term treatment, namely motor fluctuations and dyskinesias (Cenci and Konradi, 2010; Jenner, 2008; Murer and Moratalla, 2011). Pramipexole, on the other hand, while showing less potency in the improvement of motor symptomatology, is less prone to the development of motor complications and might delay and reduce them when used initially in monotherapy in "*de novo*" patients (Holloway et al., 2004; Parkinson Study Group, 2002, 2000). In addition, for a long time, a controversy on the existence of differential effects on the survival of remaining DA neurons, between these two drugs, has divided the opinions of experts in the field. Levodopa was thought to carry the risk of promoting cell death, through the increase of oxidative by-products within remaining DA neurons, while pramipexole was proposed to have neuroprotective properties. A cumulative body of evidence has been produced that helped to dispel the concept of levodopa toxicity, (Murer et al., 1999, 1998; Olanow et al., 2004), while on the other hand has casted doubts on the putative neuroprotective properties of pramipexole (Schapira et al., 2013). Furthermore, significant behavioral, biochemical and molecular differences induced by early *versus* delayed administration of levodopa or pramipexole in hemiparkinsonian rats have been reported (Marin et al., 2014). These evidences notwithstanding, there is still much to learn in regards to the ultimate mechanism of action of these two drugs and which additional factors account for their differences in terms of clinical effects.

In recent years, much has been learned about the cascade of molecular events that are set in motion downstream of the DA receptors both in the context of denervation of the nigrostriatal system by the pathological process, and by the non-physiologic stimulation of denervated DA receptors by either DA (through exogenous replacement by levodopa) and by DA receptor agonists (Ferrario et al., 2004; Grünblatt et al., 2011; Konradi et al., 2004; Meurers et al., 2009). These pervasive changes involving stimulation of transcription factors, differential expression of genes and their corresponding proteins are believed to be responsible for some of the enduring changes that underlie the development of motor complications and perhaps for their putative neuroprotective or disease modifying effects. Here we looked at the whole striatal transcriptome to characterize the gene expression patterns underlying the therapeutic effects of chronic treatments with levodopa or pramipexole in rats with nigrostriatal lesions.

2. Materials and methods

2.1. Animals

Male Wistar rats weighing 200–220 g at the beginning of the experiments were purchased from Facultad de Farmacia y Bioquímica, Universidad de Buenos Aires (Buenos Aires, Argentina). Rats were caged in groups of three or four, with free access to food and tap water in a temperature-controlled room (20 ± 2 °C) with a 12 h light/dark cycle (light period from 8 a.m. to 8 p.m.). All surgical procedures were performed in accordance with European Union Directive 2010/63/EU guidelines for the use and care of laboratory animals, as well as Argentine regulations (RS617/2002, Servicio Nacional de Sanidad y Calidad Agroalimentaria, SENASA, Argentina). All studies complied with the ARRIVE guidelines. All efforts were made to minimize animal suffering and to reduce the number of animals used.

2.2. Drugs

Commercially available Levodopa/carbidopa 250/25 mg (Lebocar, Pfizer SRL, Argentina) and Pramipexole 1 mg (Sifrol, Boehringer-Ingelheim, Germany) were dissolved in tap water as vehicle, filtered, and made available to rats in light protected bottles. This was the animals' only source of fluid and was prepared three times a week. The stability of levodopa in tap water was determined in a previous work (Ferrario et al., 2004). The concentration of the pramipexole solution remained unaltered after four days in tap water as determined by high-performance liquid chromatography (not shown). To keep the doses constant during the three weeks of treatment, drug concentration was readjusted to the mean weight of the animals and the volume of liquid they drank (Datla et al., 2001; Ferrario et al., 2004).

2.3. Intrastriatal 6-hydroxydopamine lesion

In order to produce a protracted extensive degeneration of the nigrostriatal pathway, an intrastriatal 6-OHDA injection was performed following a protocol described by Kirik et al. (1998) with slightly variations. Under deep anesthesia with ketamine/xylazine 60/10 mg/kg, respectively (Ketamina 50, Holliday–Scott, Argentina and Xylazine, Kensol, König, Argentina), rats received three stereotaxic injections of 8 μg of 6-hydroxydopamine hydrobromide (calculated as free base) (6-OHDA, MP Biochemicals, USA) dissolved in 3 μl of 0.02% ascorbic acid in saline in the left striatum with a 30-gauge steel cannula (lesioned group, LES). The dose used was selected on the basis of experience from previous experiments (not shown). A group of control rats received vehicle (0.02% ascorbic acid in saline) instead of 6-OHDA (SHAM group). The injection rate was 0.55 μl/min and the cannula was left in place for additional 3 min before slowly retracting it. Stereotaxic coordinates from bregma (mm) were: (1): 1.0 anterior, 3.0 lateral, 5.0 ventral; (2): 0.1 posterior, 3.7 lateral, 5.0 ventral; (3): 1.2 posterior, 4.5 lateral, 5.0 ventral. Rats were placed on a heating pad to minimize hypothermia until they recovered from anesthesia.

2.4. Behavioral evaluation

Akinesia of the contralateral forepaw was assessed in limb-use asymmetry tests, the cylinder test (Schallert et al., 2000) and the stepping test (Olsson et al., 1995). In the cylinder test a rat is placed in a transparent acrylic cylinder (20 cm diameter, 30 cm height) and the observer counts the number of wall contacts performed with the left, right, or both forelimbs simultaneously, during 5 min of spontaneous vertical exploration. An asymmetry score was calculated as percentage of the number of contralateral forelimb wall contacts plus 1/2 the number of both forelimbs wall contacts, divided by the total number of wall contacts (ipsilateral plus contralateral plus both forelimb contacts) (Larramendy et al., 2008; Woodlee et al., 2005). The cylinder test was performed three days before and two weeks after surgery in order to select the successfully lesioned animals. On the third week of the pharmacological treatments this test was carried out from 10 p.m. to 6 a.m., period of maximum activity of animals and maximum consumption of the drugs solution. The stepping test was conducted twice a day for three consecutive days (the animals were handled during 2 days to become familiar with the manipulation). The rat was held in one hand fixing the hindlimbs whereas one of the forelimbs was slightly fixed with the other hand. In this position and with the other forepaw touching the surface of a table of 90 cm, the rat was moved in 5 s, first to the forehand and then to the backhand direction. The number of adjusting steps was counted in both directions for each forelimb and a mean value was obtained by averaging the number of steps observed across the six sessions (theoretical maximum score per session: 16). Abnormal involuntary movements or "dyskinesias" were measured as previously described using the following scale: 0: absent; 1: occasional; 2: frequent; 3: continuous interrupted by sensory distraction; 4: continuous not interrupted by sensory distraction (Cenci and Lundblad, 2007; Delfino et al., 2004; Larramendy et al., 2008; Lundblad et al., 2004).

2.5. Tissue preparation for immunohistochemistry

Rats were anesthetized with ketamine/xylazine (60/10 mg/kg, i.p.) and perfused transcardially with 100 ml of saline followed by 250 ml of 4% paraformaldehyde in 0.1 M phosphate-buffered saline (PBS). Brains were post-fixed for 2 h in the same fixative solution, cryoprotected in 30% sucrose in 0.1 M PBS for 48 h and stored at 4 °C until sectioning. Serial coronal, 40-μm-thick tissue sections of striatum and *substantia nigra pars compacta* (SNpc) were cut in a freezing microtome. The slices were stored in PBS containing 0.1% sodium azide at 4 °C. Animals under three weeks of pharmacological treatment were perfused after a drug washout period of 24 h.

Please cite this article in press as: Taravini, I.R., et al., Contrasting gene expression patterns induced by levodopa and pramipexole treatments in the rat model of Parkinson's disease, Neuropharmacology (2015), http://dx.doi.org/10.1016/j.neuropharm.2015.04.018

2.6. Immunohistochemistry

To evaluate the severity of dopaminergic denervation in our animal model, immunohistochemistry for tyrosine hydroxylase (TH) was performed on free-floating coronal serial sections following a standard protocol (Taravini et al., 2011). During all staining procedures 0.1 M PBS containing 0.15% Triton X-100 was used for diluting all immunoreagents and for washing between all antibodies incubations. Sections were incubated in 0.3% H_2O_2 for 30 min followed by 10% normal goat serum for 30 min. The sections were incubated with the primary antiserum rabbit anti-TH (1:1000; Pel Freeze Biologicals, USA) over night at 4 °C and, after washing, with the biotin-labeled anti-rabbit IgG antiserum (1:250, Vector Laboratories, USA) for two hours. The presence of the primary antibody was visualized by means of an avidin-biotin peroxidase complex (1:125, Vectastain, ELITE ABC kit, Vector Laboratories), developed with 0.5 mg/ml 3,3'-diaminobenzidine tetrahydrochloride (Sigma, USA) and 0.015% H_2O_2.

2.7. Quantification

To determine the extent of dopaminergic denervation, the presence of TH-immunoreactive (TH-ir) cells was evaluated on the lesioned and non-lesioned hemisphere. The proportion of TH-ir cells remaining in the SNpc injected with 6-OHDA or vehicle was estimated from direct counts on nigral sections using the software Mercator Pro (Explora Nova, France). TH-ir neurons were blindly counted using a 40× objective in the ipsilateral and contralateral SNpc of four 40-μm thick coronal section (4.80, 5.30, 5.80 and 6.04 mm posterior to bregma) (Paxinos and Watson, 1986; Taravini et al., 2011). The sum of TH-ir neurons in the four nigral levels was expressed as a percentage with respect to the contralateral SNpc. The percentage of TH-ir area was determined on the lesioned striatum on every tenth 40-μm thick coronal section (a total of seven sections covering the striatum between 1.6 and −1.3 mm related to bregma) (Paxinos and Watson, 1986; Taravini et al., 2011). Optical density measurements were performed using the National Institutes of Health ImageJ software (http://rsbweb.nih.gov/ij/, NIH, USA).

2.8. Striatal dissection

After 3 weeks of daily drug administration and a washout period of 24 h, rats were exposed to carbon dioxide until loss of consciousness was achieved, and were immediately sacrificed by decapitation. Brains were quickly removed on a cold surface, striata ipsilateral to the lesion (or the left striatum of normal animals) were dissected out, immediately frozen and stored at −70 °C until total RNA isolation. The ventral mesencephalon containing the SNpc was post-fixed by immersion in 4% paraformaldehyde in 0.1 M PBS for eight hours, cryoprotected in 30% sucrose in 0.1 M PBS and sectioned in a freezing microtome. Serial coronal, 40-μm-thick tissue sections of SNpc were obtained to evaluate the extent of dopaminergic denervation by means of TH immunohistochemistry.

2.9. Preparation of RNA and microarray hybridization

Total RNA was isolated from the striatum with a commercially available kit (Qiagen RNeasy Lipid Tissue Mini kit, Qiagen, Germany), according to the manufacturer's instructions. RNA concentration and purity was determined by UV spectrophotometry measuring the ratio of the absorbencies at 260 nm and 280 nm ($A_{260/280}$) and RNA integrity was confirmed on denaturing formaldehyde 1.2% agarose gel visualizing the 18S and 28S ribosomal RNA bands. The samples passing quality control criteria (concentration ≥0.5 μg/μl and $A_{260/280}$: 1.8–2.2) were used for further analysis and stored at −70 °C until use. One hundred ng of total RNA were processed and hybridized to the Rat Genome 1.0 ST GeneChip® Array (Affymetrix, Santa Clara, CA), washing and staining procedures were carried out according to standard protocols and following the manufacturer's instructions (www.Affymetrix.com). This array allows studying the gene expression level of the whole rat genome.

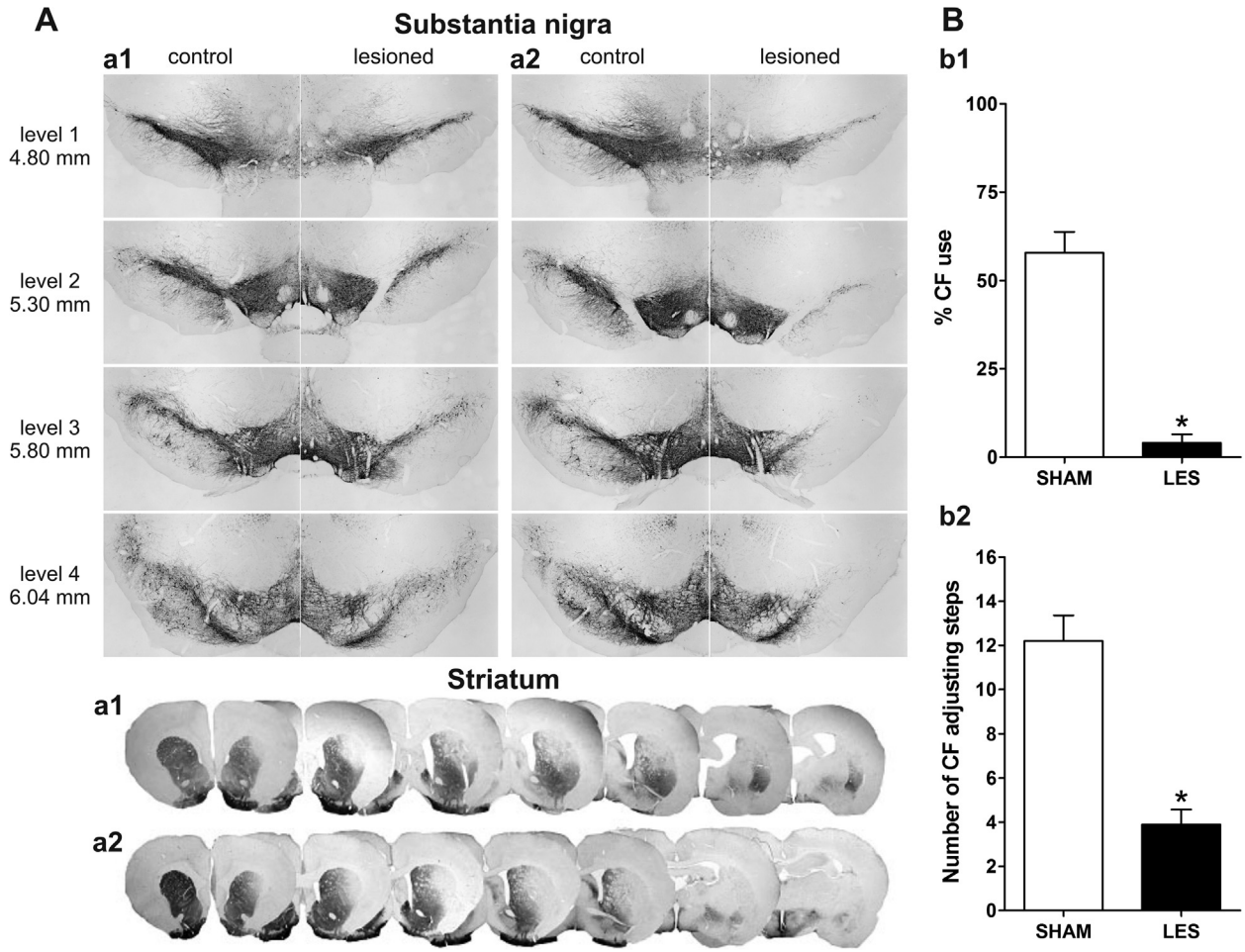

Fig. 1. Characterization of PD animal model. **A**. Tyrosine hydroxylase (TH) immunohistochemistry revealed a moderate nigrostriatal lesion after unilateral 6-OHDA injections in the striatum. Figure shows two representative animals with 47% (**a1**) and 20% (**a2**) of TH-immunoreactive (TH-ir) remaining cells at *substantia nigra pars compacta* (4.80, 5.30, 5.80 and 6.04 mm posterior to bregma) and the concomitant loss of TH-ir terminals at the striatum. **B**. Successfully 6-OHDA lesioned rats showed marked deficits in the use of the contralateral forelimb (CF) both in the cylinder test (**b1**) and the stepping test (**b2**). Data are mean ± SEM of 10 6-OHDA-lesioned rats (LES) and 5 control rats (SHAM). Nonparametric Mann–Whitney test for independent samples $^*p < 0.05$.

Please cite this article in press as: Taravini, I.R., et al., Contrasting gene expression patterns induced by levodopa and pramipexole treatments in the rat model of Parkinson's disease, Neuropharmacology (2015), http://dx.doi.org/10.1016/j.neuropharm.2015.04.018

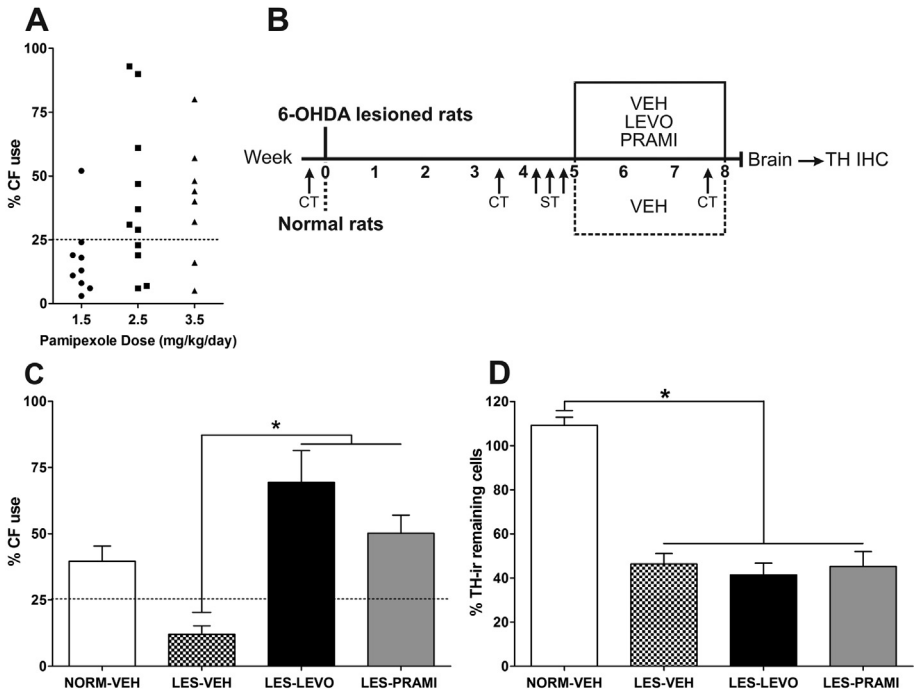

Fig. 2. Therapeutic effects of chronic levodopa and pramipexole treatments. **A**. Three groups of 6-OHDA lesioned animals were used to establish the therapeutic dose of pramipexole by means of the cylinder test (CT). Motor improvement was determined as percentage of contralateral forelimb (CF) use above 25%, as animals selected for the experiment used the CF less than 25% of the times due to the akinesia induced by the 6-OHDA lesion. The percentage of animals with CF use above 25% was 11% for the 1.5 mg/kg/day dose (n = 9), 63% for the 2.5 mg/kg/day dose (n = 11) and 75% (n = 8) for the 3.5 mg/kg/day dose. **B**. Time course of an experiment designed to compare the therapeutic effects of the 3.5 mg/kg/day pramipexole dose and a 170 mg/kg/day dose of levodopa previously used by our group (Ferrario et al., 2004). **C**. The 3.5 mg/kg/day dose of pramipexole induced comparable motor improvement to the 170 mg/kg/day dose of levodopa in the last evaluation in the CT (Kruskal Wallis test followed by multiple comparison *post hoc* Dunn test, *p < 0.05, mean ± SEM). **D**. No significant differences were observed in the percentage of remaining tyrosine hydroxylase-immunoreactive (TH-ir) cells in the *substantia nigra pars compacta* between 6-OHDA-lesioned (LES) rats treated with vehicle (VEH, n = 6), pramipexole (PRAMI, n = 6) or levodopa (LEVO, n = 6) (One way ANOVA and multiple comparison *post hoc* Tukey test, *p > 0.05). As expected, 6-OHDA-lesioned rats differed significantly from normal rats treated with vehicle (NORM-VEH, n = 5) (Tukey test, *p < 0.05, mean ± SEM). ST: Stepping test, IHC: Immunohistochemistry.

Each chip comprises more than 722,000 unique 25-mer oligonucleotide probes (median of 26 probes per gene) represented by more than 27,300 distinct probes. This analysis was performed on samples from three pools of four rat striata per group: lesioned treated with, vehicle (LES-VEH), levodopa (LES-LEVO) or pramipexole (LES-PRAMI) and normal rats treated with vehicle (NORM-VEH), resulting in a total of 12 chips.

2.10. Microarray analysis

Raw data was normalized and summarized at gene level by means of the Robust Multichip Analysis (Carvalho et al., 2007) method from oligo package (Carvalho and Irizarry, 2010). Then, quality control assessment was performed in order to remove bad quality probes from further analysis. Differential expression analysis was carried out fitting a linear model for each gene and comparing the conditions of interest using the appropriate contrasts, as implemented in limma package (Smyth, 2005). Genes were considered differentially expressed if they show a p value <0.05 and a log2 fold change >0.3 (McCarthy and Smyth, 2009).

Hierarchical clustering analysis (Wilkinson and Friendly, 2009) was applied on differentially expressed genes to compare expression patterns across treatments, using Euclidean distance as the dissimilarity metric and complete linkage as the agglomeration method. The results of these analyses were displayed using a "heat map" where signal intensity of differentially expressed genes is mapped to a color scale and clustering is applied on both rows and columns. All of the methods used in this section are implemented as R packages and freely available at www.bioconductor.org.

2.11. Quantitative real-time RT-PCR

Using the same RNA samples prepared for the microarray hybridization, we attempted to validate the expression of nine selected genes by quantitative real-time RT-PCR (qRT-PCR), using the 7500 Real-Time PCR System (Applied Biosystems, Foster City, CA). The procedure was performed in one step using a commercially available kit (Power SYBR® Green RNA-to-Ct™ 1-step), according to the manufacturer's instructions (Applied Biosystems). RNA was amplified in a total volume PCR reaction mixture of 12.5 μl with specific primers for Nr4a2 (Nurr1, *nuclear receptor subfamily 4, group A, member 2*), Psmd14 (*proteasome (prosome, macropain) 26S subunit, non-ATPase, 14*), Ndufa12 (*NADH dehydrogenase (ubiquinone) 1 alpha subcomplex, 12*), Olr1375 (*olfactory receptor 1375*), Ppp1r2 (*Protein phosphatase inhibitor 2*), Gabarap (*Gamma-aminobutyric acid receptor-associated protein*), Mybl1 (*myeloblastosis oncogene-like 1*), Sod1 (*superoxide dismutase 1*) (Eurofins Scientific, Luxembourg) and, GFAP (*glial fibrillary acidic protein*). The sequences of the primers are given in Supplementary Table 1. Expression of each target gene was normalized using values obtained either HPRT (Hypoxanthine-guanine phosphoribosyltransferase) or GAPDH (Glyceraldehyde 3-phosphate dehydrogenase) and relative to the control groups was calculated using the ΔΔCT method (Livak and Schmittgen, 2001). Each sample was analyzed in triplicate and appropriate negative controls (no-template) were also run on each plate in triplicate. Data were analyzed using sequence detection systems software 7500 v.2.0.3 (Applied Biosystems). Results were expressed as relative levels of target gene in the treated referred to control samples.

3. Results

3.1. Validation of clinically effective levodopa and pramipexole oral treatments in a model of early PD

To simulate an early stage of PD, partial lesions of the nigrostriatal system were induced by injecting 6-OHDA at multiple sites in the left striatum (Fig. 1A). Animals showing marked spontaneous behavioral deficit as assessed by the cylinder and stepping tests (Fig. 1B) were selected for further pharmacological studies. First, we tested the effect of different doses of pramipexole dissolved in tap water (vehicle) in the cylinder test (Fig. 2A). A 1.5 mg/kg/day dose induced no benefit whereas 2.5 and 3.5 mg/kg/day doses induced similar behavioral improvement (8–11 rats per group). Then, in a new set of 6-OHDA lesioned rats, we compared the behavioral improvement induced by pramipexole with that induced by a previously validated oral levodopa treatment (Ferrario et al., 2004).

Please cite this article in press as: Taravini, I.R., et al., Contrasting gene expression patterns induced by levodopa and pramipexole treatments in the rat model of Parkinson's disease, Neuropharmacology (2015), http://dx.doi.org/10.1016/j.neuropharm.2015.04.018

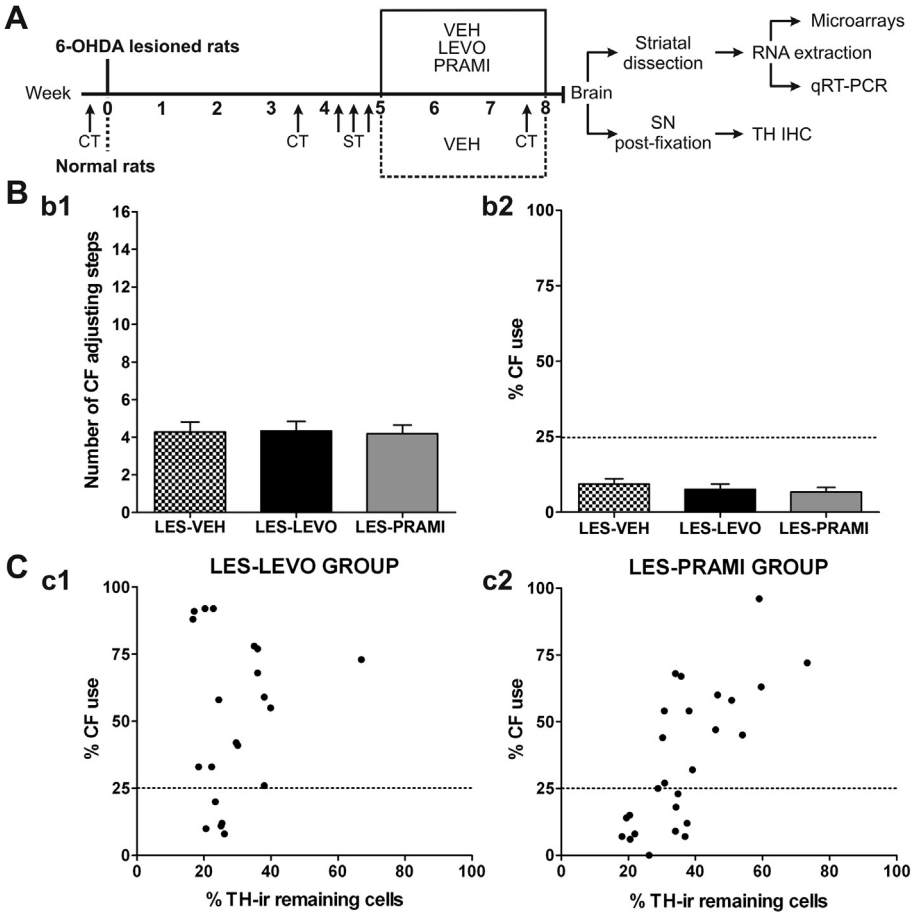

Fig. 3. Correlation between symptomatic amelioration induced by the pharmacological treatments and degree of nigrostriatal damage. **A**. Experimental design of the pharmacological regimes with pramipexole (3.5 mg/kg/day) or levodopa (170 mg/kg/day) and behavioral evaluation (cylinder test, CT; stepping test, ST). **B**. 6-OHDA lesion induced similar behavioral deficits in the use of the contralateral forelimb (CF) both in the CT (**b1**) and the ST (**b2**) in the three groups of lesioned rats (LES) which received vehicle (VEH, n = 18), levodopa (LEVO, n = 21) or pramipexole (PRAMI, n = 26). **C**. Graph showing the degree of behavioral improvement *versus* the percentage of tyrosine hydroxylase-immunoreactive (TH-ir) neurons remaining in the *substantia nigra pars compacta* after treatment with levodopa (**c1**) or pramipexole (**c2**). Pearson correlation analyses of these variables show a clear correlation for pramipexole ($r = 0.73$, $p < 0.0001$) but not for levodopa treatment ($r = 0.13$, $p = 0.59$). SN: *substantia nigra*, qRT-PCR: quantitative real-time RT-PCR, IHC: Immunohistochemistry.

Vehicle (n = 6), levodopa/carbidopa (170/17 mg/kg/day, n = 6) or pramipexole (3.5 mg/kg/day, n = 6) were administered for three weeks to 6-OHDA lesioned animals according to the protocol depicted in Fig. 2B. Both treatments induced a significant improvement in the cylinder test and did not differ from each other (Fig. 2C). Importantly, abnormal involuntary movements or dyskinesias were looked for independently by two trained observers (CL and IT) and were not found in any of the animals regardless of treatment. Postmortem studies showed ~60% depletion of TH-ir neurons in the SNpc of 6-OHDA lesioned animals (Fig. 2D). Overall the data show that oral pramipexole and levodopa at the selected doses induce a similar degree of behavioral improvement without inducing dyskinesias in a partial lesion model of PD, similar to what happens in patients at the early stages of PD (Holloway et al., 2004; Parkinson Study Group, 2009, 2000).

3.2. Correlation between treatment-induced symptomatic amelioration and degree of nigrostriatal damage

From a new set of 6-OHDA lesioned rats showing clear behavioral deficits we obtained, by random sampling, three experimental groups which were assigned to receive either vehicle (n = 18), levodopa/carbidopa (170/17 mg/kg/day; n = 21) or pramipexole (3.5 mg/kg/day; n = 26) for three weeks (Fig. 3A). *Post hoc* analysis confirmed similar lesion-induced behavioral deficits in the three groups of 6-OHDA rats (Fig. 3B). However, when the degree of behavioral improvement was plotted against the percentage of TH-ir neurons remaining in the SNpc (Fig. 3C), a clear correlation was found for pramipexole only ($r = 0.73$, $p < 0.0001$), where the higher the nigral cell loss, the lower the symptomatic effect of pramipexole.

3.3. Contrasting gene expression patterns induced by levodopa and pramipexole treatments

From the animal set described in Fig. 3, three groups of 6-OHDA-lesioned rats (n = 12 each), which received either vehicle, levodopa/carbidopa (170/17 mg/kg/day) or pramipexole (3.5 mg/kg/day) for three weeks and were randomly selected for the microarray experiments. In parallel, twelve control (non-lesioned) rats received vehicle alone (as described in Fig. 3A). In order to run the microarray experiment in triplicate, each experimental group was further divided into 3 subgroups of four animals each (Fig. 4A). *Post hoc* analysis confirmed similar lesion-induced behavioral deficits in all the subgroups of 6-OHDA rats (Fig. 4B). As expected, both pharmacological treatments induced similar symptomatic

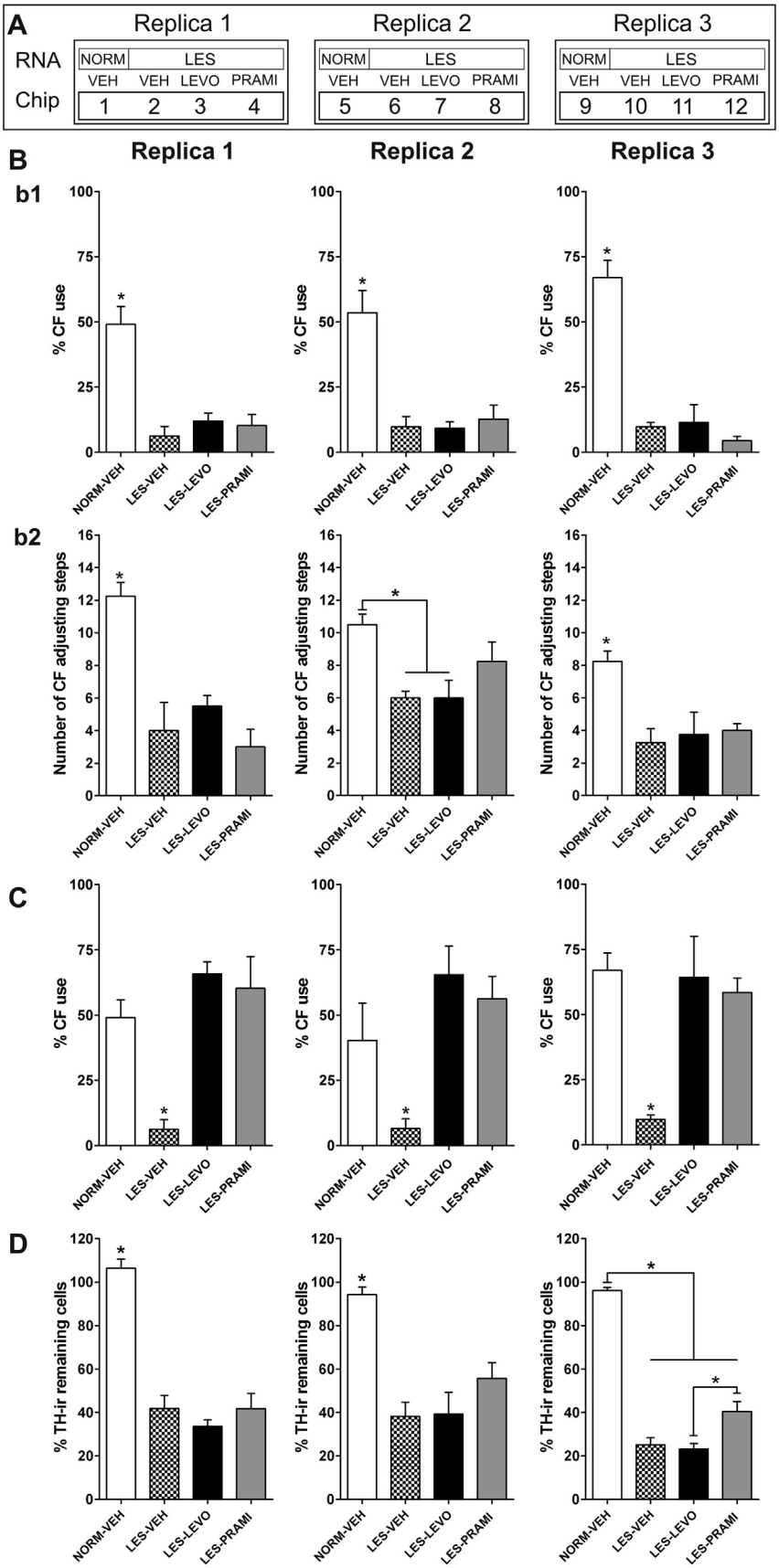

Fig. 4. Behavioral evaluation of hemiparkinsonian rats under pharmacological treatment. **A**. The microarray experiment was performed in triplicate. After the pharmacological treatment each experimental group was further subdivided in 3 groups (replicas) of 4 animals each. Normal-vehicle (NORM-VEH), lesioned-vehicle (LES-VEH), lesioned-levodopa (LES-LEVO) and lesioned-pramipexole (LES-PRAMI). **B**. Lesioned animals presented comparable behavioral deficits in the use of the contralateral forelimb (CF) both in the cylinder

Please cite this article in press as: Taravini, I.R., et al., Contrasting gene expression patterns induced by levodopa and pramipexole treatments in the rat model of Parkinson's disease, Neuropharmacology (2015), http://dx.doi.org/10.1016/j.neuropharm.2015.04.018

Table 1
Genes differentially expressed in response to levodopa or pramipexole treatments. Differences were considered statistically significant at a level of $p < 0.05$. Number of genes differentially expressed with a minimum fold change of 0.3 for each comparison between treatments.

Fold change $\geq$0.3 or $\leq$−0.3 and $p < 0.05$	
Comparison	N° of Genes
LES-LEVO vs LES-VEH	240
LES-PRAMI vs LES-VEH	189
LES-LEVO vs LES-PRAMI	550

amelioration in rats belonging to each replica (Fig. 4C). Postmortem cell counts revealed a significantly higher number of remaining TH-ir nigral neurons in the pramipexole-treated animals of one of the replicas (Fig. 4D). This is probably related to the fact that the therapeutic effect of pramipexole is inversely related to degree of nigral neuron depletion (Fig. 3D), resulting in the exclusion of severely lesioned animals from the pramipexole treated group because of the lack of therapeutic effect.

Gene expression analysis was performed with Affymetrix microarray encompassing the whole rat transcriptome (see Section 2.9). Overall, the treatments produced relatively small quantitative changes in a large number of genes (Table 1). Setting threshold at 0.3 fold change, levodopa induced significant ($p < 0.05$) expression changes in 240 genes and pramipexole in 189 genes, when compared to vehicle alone (Supplementary Table 2). Among them, only 23 genes suffered significant changes with both treatments (Fig. 5), indicating that different gene expression patterns lie behind the levodopa and pramipexole therapeutic effects.

Furthermore, when levodopa was compared to pramipexole 550 genes showed a significant >0.3 fold change (Supplementary Table 2), among which 402 were not present in the comparison of each treatment against vehicle (Fig. 5). Thus, only 100 of the 240 genes identified in the levodopa *versus* vehicle comparison and 47 of the 189 genes identified in the pramipexole *versus* vehicle comparison were present in the levodopa/pramipexole comparison. This is because levodopa and pramipexole have small but opposite effects on a number of transcripts, which did not stand as significant when taking vehicle as reference but come out as different when the treatments are directly compared against each other.

Heat maps on differentially expressed genes showed consistent effects of the treatments across replicas (Fig. 5), providing evidence for the reproducibility of the sampling and quantification procedures. Moreover, despite the overall small size of changes in mRNA expression at the level of individual transcripts, it revealed a robust and complete segregation of the treatments in comparisons against vehicle (Fig. 5A and B) and against each other (Fig. 5C).

3.4. Ribosomal and mitochondrial related transcripts distinguish levodopa from pramipexole treatment

The gene expression patterns induced by the treatments were further characterized by studying the enrichment of differentially expressed genes within specific molecular pathways following the Kyoto Encyclopedia of Genes and Genomes (KEGG, http://www.genome.jp/kegg/) (Werner, 2008). The KEGG database is organized in pathways linking sets of transcripts with normal and pathological cellular processes. Six KEGG pathways are enriched with transcripts detected in the comparison levodopa against vehicle (Table 2): olfactory transduction (22 transcripts), ribosome (18 transcripts), Parkinson's disease (7 transcripts), oxidative phosphorylation (6 transcripts), proteasome (2 transcripts) and Huntington's disease (7 transcripts). Only one pathway, olfactory transduction, is enriched with transcripts (19) in the pramipexole against vehicle comparison. Finally, enrichment of olfactory transduction (24 transcripts), ribosome (20 transcripts), oxidative phosphorylation (12), Parkinson's disease (12), Huntington's disease (14) and proteasome (5) pathways distinguish levodopa from the pramipexole treatment. Some of these pathways are highly related to each other, sharing transcripts related to oxidative phosphorylation and oxidative stress (Table 2), whose expression is primarily modified by levodopa administration.

3.5. Validation of microarray data by qRT-PCR

In order to validate the microarray results, we performed qRT-PCR analysis of nine transcripts, which were selected based on their enrichment in the above KEGG pathways, the magnitude of the fold change observed in the microarray experiment, or previous reports showing expression changes in PD patients or animal models of PD. Table 3 shows a comparison between microarray and qRT-PCR results. Among a total of 21 comparisons, only two gave qualitatively opposite changes with qRT-PCR compared to the microarray results. Except for these two comparisons, changes observed with the microarray were linearly related to changes observed with qRT-PCR ($r = 0.72$, slope $= 0.46$, $p < 0.0006$; Fig. 6).

4. Discussion

High throughput analysis techniques, such as transcriptomics, provide an unbiased approach to the detection of a set of analytes that can differentiate between conditions in a biological sample. In this experiment we have used this approach in an attempt to differentiate the expression profile of the whole rat transcriptome by means of a microarray applied to the striatum of a rat model of early PD undergoing two different treatment regimens with either levodopa or pramipexole in clinically meaningful doses. The results obtained confirmed our assumption that given the different pharmacokinetic and pharmacodynamic profiles, as well as their different clinical effects, these two commonly used anti-parkinsonian drugs would induce a significantly different gene expression profile.

Our data strongly validate the use of partial 6-OHDA-induced nigrostriatal lesions to model early stage PD. This is illustrated by the reproduction of the long-discussed effect of disease progression on D2 agonist therapeutic action often observed in clinical settings (Pd Med Collaborative Group, 2014). In our animals there was a marked correlation between the number of remaining dopaminergic neurons in the substantia nigra and the therapeutic effect induced by pramipexole (but not levodopa), so that animals with extensive degeneration show little response to pramipexole (Fig. 3C). The reduction of the therapeutic benefit obtained with D2 agonists as disease progresses is usually attributed to the loss of concomitant endogenous D1 receptor stimulation as dopaminergic

test (**b1**) and the stepping test (**b2**). **C**. Cylinder test under treatment. Percentage of CF use under pharmacological treatment of selected animals for microarray experiment for each replica (n = 4 per group per replica). **D**. No significant differences were observed in the percentage of remaining tyrosine hydroxylase-immunoreactive (TH-ir) cells in the *substantia nigra pars compacta* between 6-OHDA-lesioned rats treated with vehicle, pramipexole or levodopa except in the third replica where the percentage of remaining TH-ir nigral neurons was significantly higher in pramipexole-treated than in levodopa-treated animals. Lesioned rats differed significantly from normal rats treated with vehicle (One way ANOVA and Tukey's multiple comparison test, $^{*}p < 0.05$, mean ± SEM).

Please cite this article in press as: Taravini, I.R., et al., Contrasting gene expression patterns induced by levodopa and pramipexole treatments in the rat model of Parkinson's disease, Neuropharmacology (2015), http://dx.doi.org/10.1016/j.neuropharm.2015.04.018

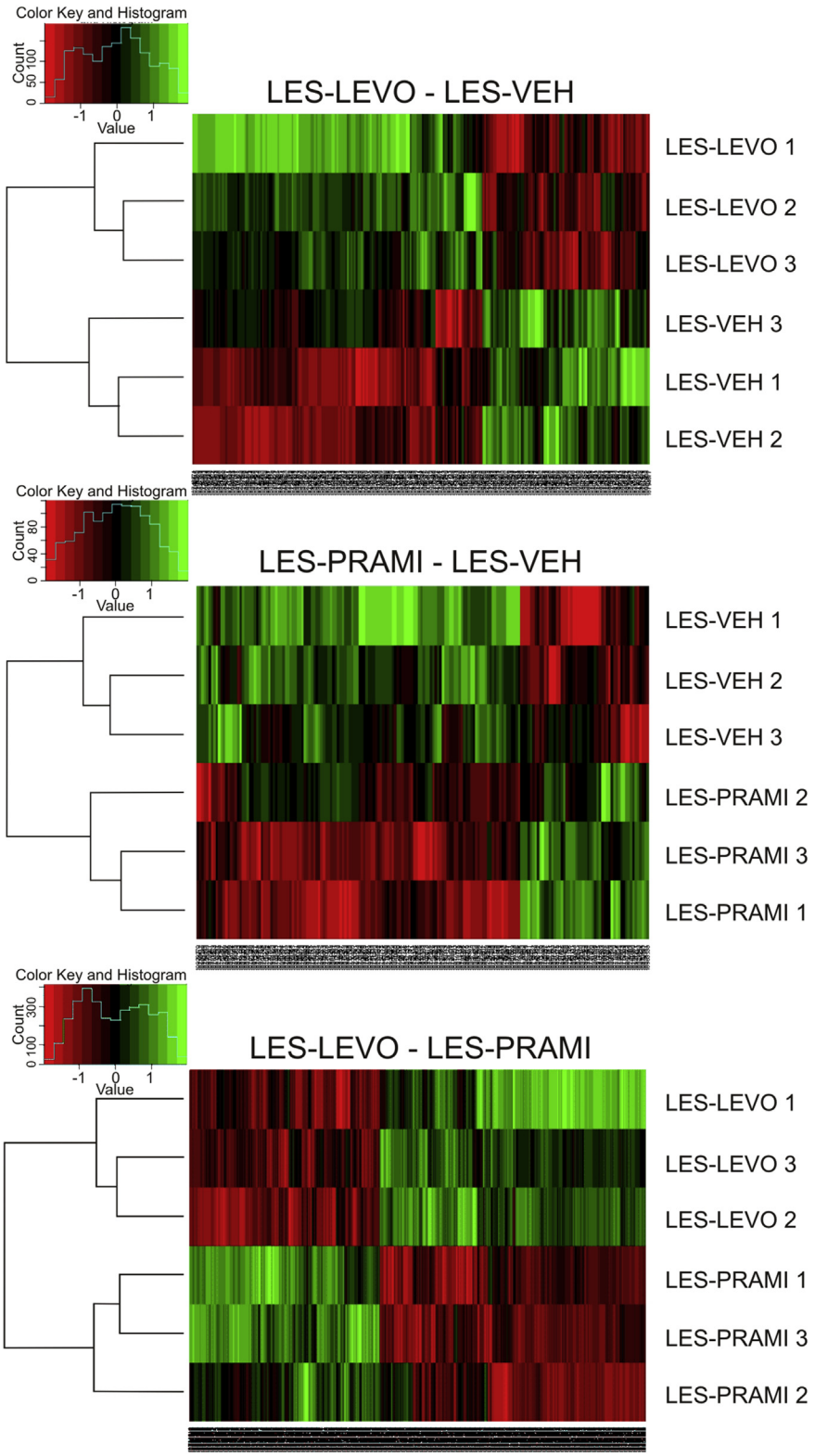

Fig. 5. Heat maps showing the genes expression levels induced by levodopa or pramipexole in the striatum of 6-OHDA lesioned rats. Vertical rows represent individual genes and horizontal rows represent a chip or biological replica for each treatment. Each cell in the matrix represents the expression level of a single transcript, with green and red indicating transcript level above and below the median level of expression for that gene, respectively and the rest color codes fall in between. The three horizontal rows at the top of each heat map are replicas of the same condition, while the three horizontal rows at the bottom are replicas of another condition. The depicted hierarchical cluster dendrograms at the left of the heat maps indicate the level of correspondence between two or more conditions based on the expression levels of differentially expressed genes.

Please cite this article in press as: Taravini, I.R., et al., Contrasting gene expression patterns induced by levodopa and pramipexole treatments in the rat model of Parkinson's disease, Neuropharmacology (2015), http://dx.doi.org/10.1016/j.neuropharm.2015.04.018

Table 2
Functional analysis of modified gene expression after pharmacological treatments. Kyoto Encyclopedia of Gene and Genome (KEGG) database was used to define functions and pathways modified in the lesioned striatum of rats treated with levodopa, pramipexole or vehicle. KEGG pathways were selected with an adjusted $p < 0.05$. This analysis highlighted six KEGG pathways: olfactory transduction, ribosome, Parkinson's disease, oxidative phosphorylation, proteasome and Huntington's disease. LV: Lesioned-Vehicle, LL: Lesioned-Levodopa, LP: Lesioned-Pramipexole.

Gene Symbol	Gene Description	LL vs LV	LP vs LV	LL vs LP
KEGG: rno04740: Olfactory transduction				
Olr46	olfactory receptor 46	−0.388		
Olr80	olfactory receptor 80		−0.307	
Olr210	olfactory receptor 210	−0.465		
Olr252	olfactory receptor 252		−0.314	
Olr285	olfactory receptor 285	−0.430		
Olr292	olfactory receptor 292	−0.406		
Olr311	olfactory receptor 311		−0.337	0.462
Olr315	olfactory receptor 315			0.447
Olr318	olfactory receptor 318			0.308
Olr385	olfactory receptor 385		0.426	−0.400
Olr401	olfactory receptor 401		−0.358	
Olr476	olfactory receptor 476			−0.364
Olr484	olfactory receptor 484			0.302
Olr490	olfactory receptor 490	−0.474	−0.465	
Olr491	olfactory receptor 491			0.349
Olr561	olfactory receptor 561	−0.354		
Olr566	olfactory receptor 566		−0.510	
Olr576	olfactory receptor 576	−0.350		
Olr581	olfactory receptor 581		−0.540	
Olr590	olfactory receptor 590		−0.377	
Olr607	olfactory receptor 607	−0.428		
Olr630	olfactory receptor 630			0.334
Olr640, Olr637, Olr635, Olr624, Olr633	olfactory receptor 640, olfactory receptor 637, olfactory receptor 635, olfactory receptor 624, olfactory receptor 633	0.337		
Olr663	olfactory receptor 663			0.344
Olr664	olfactory receptor 664	−0.372		
Olr666	olfactory receptor 666	0.307		0.359
Olr673	olfactory receptor 673	0.416		
Olr715	olfactory receptor 715	0.479		
Olr735	olfactory receptor 735			0.302
Olr736	olfactory receptor 736	0.333		
Olr748	olfactory receptor 748			0.410
Olr769	olfactory receptor 769			0.433
Olr785	olfactory receptor 785			−0.584
Olr789	olfactory receptor 789		0.455	
Olr838	olfactory receptor 838		−0.372	
Olr838	olfactory receptor 838			0.305
Olr848, Olr844, Olr845, Olr850	olfactory receptor 848, olfactory receptor 844, olfactory receptor 845, olfactory receptor 850	−0.398	−0.303	
Olr844, Olr848, Olr845, Olr850, Olr847	olfactory receptor 844, olfactory receptor 848, olfactory receptor 845, olfactory receptor 850, olfactory receptor 847	−0.450	−0.318	
Olr869	olfactory receptor 869	−0.532		
Olr1082	olfactory receptor 1082		0.329	
Olr1122	olfactory receptor 1122			−0.305
Olr1248, Olr1247, Olr1249, Olr1246	olfactory receptor 1248, olfactory receptor 1247, olfactory receptor 1249, olfactory receptor 1246	−0.305		
Olr1259	olfactory receptor 1259			−0.498
Olr1288	olfactory receptor 1288		−0.308	0.359
Olr1325	olfactory receptor 1325	0.730		0.660
Olr1361	olfactory receptor 1361			−0.310
Olr1375	olfactory receptor 1375		−0.541	
Olr1380	olfactory receptor 1380	−0.371		
Olr1382	olfactory receptor 1382		−0.333	0.342
Olr1425	olfactory receptor 1425			−0.309
Olr1627	olfactory receptor 1627			0.324
Olr1641	olfactory receptor 1641			0.637
Olr1654	olfactory receptor 1654		0.646	
Olr1687	olfactory receptor 1687	−0.315		
Olr1746	olfactory receptor 1746	−0.374		
RGD1561276	similar to olfactory receptor Olfr1289		0.338	
Number of genes		**22**	**19**	**24**
KEGG: rno05012: Parkinson's disease				
Cox5a	cytochrome c oxidase, subunit Va	0.353		0.347
Cox5a	cytochrome c oxidase, subunit Va			0.391
Cox6a1	cytochrome c oxidase, subunit VIa, polypeptide 1			0.329
Cox7a2l	cytochrome c oxidase subunit VIIa polypeptide 2 like			0.328
Htra2	HtrA serine peptidase 2			0.385
ND6	NADH dehydrogenase subunit 6	0.672		
Ndufa6	NADH dehydrogenase (ubiquinone) 1 alpha subcomplex, 6 (B14)			0.334

(*continued on next page*)

Please cite this article in press as: Taravini, I.R., et al., Contrasting gene expression patterns induced by levodopa and pramipexole treatments in the rat model of Parkinson's disease, Neuropharmacology (2015), http://dx.doi.org/10.1016/j.neuropharm.2015.04.018

Table 2 (*continued*)

Gene Symbol	Gene Description	LL vs LV	LP vs LV	LL vs LP
Ndufb6	NADH dehydrogenase (ubiquinone) 1 beta subcomplex, 6	0.621		0.741
Ndufc2	NADH dehydrogenase (ubiquinone) 1, subcomplex unknown, 2			0.315
Sdhc	succinate dehydrogenase complex, subunit C, integral membrane protein	0.415		0.499
Sdhd	succinate dehydrogenase complex, subunit D, integral membrane protein	0.300		
Slc25a4	solute carrier family 25 (mitochondrial carrier; adenine nucleotide translocator), member 4			0.316
Ube2g2	ubiquitin-conjugating enzyme E2G 2	0.380		
Uqcr	ubiquinol-cytochrome c reductase, 6.4 kDa subunit			0.394
Uqcrfs1	ubiquinol-cytochrome c reductase, Rieske iron–sulfur polypeptide 1	0.315		0.371
Uqcrq	ubiquinol-cytochrome c reductase, complex III subunit VII			0.370
Number of genes		**7**	**0**	**12**
KEGG: rno03010: Ribosome				
Dtna, RGD1563861	dystrobrevin alpha, similar to ribosomal protein L10	0.452		0.688
Fau, RGD1565317	Finkel-Biskis-Reilly murine sarcoma virus (FBR-MuSV) ubiquitously expressed, similar to ubiquitin-like/S30 ribosomal fusion protein			0.332
Fau, RGD1565317	Finkel-Biskis-Reilly murine sarcoma virus (FBR-MuSV) ubiquitously expressed, similar to ubiquitin-like/S30 ribosomal fusion protein			0.329
LOC499782, RGD1564883, Rpl12, RGD1563956	similar to 60S ribosomal protein L12, ribosomal protein L12			0.376
LOC688136	similar to 60S ribosomal protein L37a	0.392		
RGD1309784	similar to ribosomal protein L24-like; 60S ribosomal protein L30 isolog; my024 protein; homolog of yeast ribosomal like protein 24	0.301		
RGD1565131	similar to ribosomal protein L15	0.324		
RGD1566373	similar to large subunit ribosomal protein L36a			0.432
Rpl10	ribosomal protein L10	0.418		0.554
Rpl18a	ribosomal protein L18A	−0.387		
Rpl23a, RGD1565170	ribosomal protein L23a, similar to 60S ribosomal protein L23a			0.319
Rpl24	ribosomal protein L24	0.344		0.450
Rpl26, Rpl26-ps1	ribosomal protein L26, ribosomal protein L26, pseudogene 1	0.326		
Rpl31	ribosomal protein L31	0.314		
Rpl31, RGD1564839	ribosomal protein L31, similar to ribosomal protein L31	0.392		0.370
Rpl31, RGD1564839, LOC680384	ribosomal protein L31, similar to ribosomal protein L31	0.531		0.451
Rpl31, RGD1564839, LOC680384	ribosomal protein L31, similar to ribosomal protein L31	0.367		
Rpl31, RGD1564839, LOC680384, LOC681338	ribosomal protein L31, similar to ribosomal protein L31	0.334		0.326
Rpl31, RGD1564839, RGD1563551, LOC680384	ribosomal protein L31, similar to ribosomal protein L31	0.367		0.312
Rpl34, LOC680170	ribosomal protein L34, similar to ribosomal protein L34			0.409
Rpl34, LOC680170	ribosomal protein L34, similar to ribosomal protein L34			0.402
Rpl36a, RGD1563431	ribosomal protein L36a, similar to large subunit ribosomal protein L36a			0.315
Rpl36a, RGD1563431	ribosomal protein L36a, similar to large subunit ribosomal protein L36a			0.353
Rpl36a, RGD1563431	ribosomal protein L36a, similar to large subunit ribosomal protein L36a			0.381
Rpl37a	ribosomal protein L37a	0.332		0.312
Rpl37a	ribosomal protein L37a	0.311		
Rpl37a-ps2	ribosomal protein L37a, pseudogene 2			0.306
Rplp1, RGD1565054, LOC502350	ribosomal protein, large, P1, similar to 60S acidic ribosomal protein P1	0.313		0.316
Rplp1, RGD1565054, RGD1560815, LOC502350	ribosomal protein, large, P1, similar to 60S acidic ribosomal protein P1, similar to acidic ribosomal phosphoprotein P1	0.307		0.314
Rps12	ribosomal protein S12	0.301		0.303
Rps12	ribosomal protein S12	0.319		0.363
Rps12	ribosomal protein S12	0.350		
Rps12	ribosomal protein S12	0.377		
Rps21	ribosomal protein S21	0.393		0.578
Rps21	ribosomal protein S21	0.390		0.576
Rps21	ribosomal protein S21	0.436		0.593
Rps27a	ribosomal protein S27a	0.326		0.369
Rps27a	ribosomal protein S27a	0.344		0.385
Rps27a, RGD1560997, LOC688462	ribosomal protein S27a, similar to ribosomal protein S27a	0.354		0.387
Rps8, LOC297756, RGD1566369	ribosomal protein S8, ribosomal protein S8-like, similar to ribosomal protein S8	0.346		0.337
Rps8, LOC297756, RGD1566369	ribosomal protein S8, ribosomal protein S8-like, similar to ribosomal protein S8	0.349		
Scn7a, RGD1560831	sodium channel, voltage-gated, type VII, alpha, similar to 40S ribosomal protein S3			−0.629
Number of genes		**18**	**0**	**20**
KEGG: rno03050: Proteasome				
Psma2	proteasome (prosome, macropain) subunit, alpha type 2			0.318
Psma4	proteasome (prosome, macropain) subunit, alpha type 4			0.367
Psmb4	proteasome (prosome, macropain) subunit, beta type 4			0.353
Psmb5	proteasome (prosome, macropain) subunit, beta type 5	0.394		
Psmb5	proteasome (prosome, macropain) subunit, beta type 5			0.619
Psmd14	proteasome (prosome, macropain) 26S subunit, non-ATPase, 14	0.465		
Psmd14	proteasome (prosome, macropain) 26S subunit, non-ATPase, 14			0.502
Number of genes		**2**	**0**	**5**
KEGG: rno00190: oxidative phosphorylation				
Atp6v1f	ATPase, H transporting, lysosomal V1 subunit F			0.446
Cox5a	cytochrome c oxidase, subunit Va	0.353		0.391
Cox5a	cytochrome c oxidase, subunit Va			0.347

Please cite this article in press as: Taravini, I.R., et al., Contrasting gene expression patterns induced by levodopa and pramipexole treatments in the rat model of Parkinson's disease, Neuropharmacology (2015), http://dx.doi.org/10.1016/j.neuropharm.2015.04.018

Table 2 (*continued*)

Gene Symbol	Gene Description	LL vs LV	LP vs LV	LL vs LP
Cox6a1	cytochrome c oxidase, subunit VIa, polypeptide 1			0.499
Cox7a2l	cytochrome c oxidase subunit VIIa polypeptide 2 like			0.328
ND6	NADH dehydrogenase subunit 6	0.672		
Ndufa11	NADH dehydrogenase (ubiquinone) 1 alpha subcomplex 11			0.320
Ndufa6	NADH dehydrogenase (ubiquinone) 1 alpha subcomplex, 6 (B14)			0.334
Ndufb6	NADH dehydrogenase (ubiquinone) 1 beta subcomplex, 6	0.621		0.741
Ndufc2	NADH dehydrogenase (ubiquinone) 1, subcomplex unknown, 2			0.315
Sdhc	succinate dehydrogenase complex, subunit C, integral membrane protein	0.415		0.499
Sdhd	succinate dehydrogenase complex, subunit D, integral membrane protein	0.300		
Uqcr	ubiquinol-cytochrome c reductase, 6.4 kDa subunit			0.394
Uqcrfs1	ubiquinol-cytochrome c reductase, Rieske iron–sulfur polypeptide 1	0.315		0.371
Uqcrq	ubiquinol-cytochrome c reductase, complex III subunit VII			0.370
Number of genes		**6**	**0**	**12**
KEGG: rno05016: Huntington's disease				
Cox5a	cytochrome c oxidase, subunit Va	0.353		0.391
Cox5a	cytochrome c oxidase, subunit Va			0.347
Cox6a1	cytochrome c oxidase, subunit VIa, polypeptide 1			0.499
Cox7a2l	cytochrome c oxidase subunit VIIa polypeptide 2 like			0.328
Dnai2	dynein, axonemal, intermediate chain 2			0.309
Gpx1	glutathione peroxidase 1			0.310
Ndufa6	NADH dehydrogenase (ubiquinone) 1 alpha subcomplex, 6 (B14)			0.334
Ndufb6	NADH dehydrogenase (ubiquinone) 1 beta subcomplex, 6	0.621		0.741
Ndufc2	NADH dehydrogenase (ubiquinone) 1, subcomplex unknown, 2			0.315
Polr2f	polymerase (RNA) II (DNA directed) polypeptide F	0.322		
Sdhc	succinate dehydrogenase complex, subunit C, integral membrane protein	0.415		0.499
Sdhd	succinate dehydrogenase complex, subunit D, integral membrane protein	0.300		
Slc25a4	solute carrier family 25 (mitochondrial carrier; adenine nucleotide translocator), member 4			0.316
Sod1	superoxide dismutase 1, soluble	0.353		0.472
Uqcr	ubiquinol-cytochrome c reductase, 6.4 kDa subunit			0.394
Uqcrfs1	ubiquinol-cytochrome c reductase, Rieske iron–sulfur polypeptide 1	0.315		0.371
Uqcrq	ubiquinol-cytochrome c reductase, complex III subunit VII			0.370
Number of genes		**7**	**0**	**14**

Table 3
Comparison of paired microarray and quantitative real-time RT-PCR (qRT-PCR) assays for candidate genes. Fold changes were measured using microarray and qRT-PCR. Upregulated genes expression in the first condition *versus* the second one are shown as positive fold changes and downregulated as negative fold changes. Similar level of fold change patterns were seen for 19 of 21 comparisons from a total of nine candidate genes (although magnitudes of change were different).

Gene	Microarray		qRT-PCR
	Fold change	p	Fold change
GFAP			
LES-VEH vs NORM-VEH	1.06	0.00019	2.33
Gabarap			
LES-LEVO vs LES-PRAMI	0.38	0.00400	−0.24
Mybl1			
LES-LEVO vs LES-VEH	−0.15	0.19600	−0.17
LES-PRAMI vs LES-VEH	0.34	0.01000	0.46
LES-LEVO vs LES-PRAMI	−0.49	0.00100	−0.63
Ndufa12			
LES-LEVO vs LES-VEH	0.43	0.01600	0.03
LES-PRAMI vs LES-VEH	−0.08	0.63100	0.68
LES-LEVO vs LES-PRAMI	0.51	0.00700	−0.64
Nr4a2			
LES-LEVO vs LES-VEH	−0.08	0.65300	0.02
LES-PRAMI vs LES-VEH	0.56	0.00800	0.62
LES-LEVO vs LES-PRAMI	−0.65	0.00300	−0.60
Olr1375			
LES-PRAMI vs LES-VEH	−0.54	0.00048	1.28
Ppp1r2			
LES-LEVO vs LES-VEH	0.31	0.00400	0.21
LES-PRAMI vs LES-VEH	−0.02	0.80300	0.03
LES-LEVO vs LES-PRAMI	0.33	0.00300	0.17
Psmd14			
LES-LEVO vs LES-VEH	0.47	0.00700	0.11
LES-PRAMI vs LES-VEH	−0.04	0.80500	0.07
LES-LEVO vs LES-PRAMI	0.50	0.00400	0.04
Sod1			
LES-LEVO vs LES-VEH	0.35	0.01800	−0.09
LES-PRAMI vs LES-VEH	−0.12	0.37800	−0.22
LES-LEVO vs LES-PRAMI	0.47	0.00300	0.14

Please cite this article in press as: Taravini, I.R., et al., Contrasting gene expression patterns induced by levodopa and pramipexole treatments in the rat model of Parkinson's disease, Neuropharmacology (2015), http://dx.doi.org/10.1016/j.neuropharm.2015.04.018

cells degenerate in the substantia nigra (Dziewczapolski et al., 1997a; Robertson and Robertson, 1986; Treseder et al., 2000). But it is also suspected that patients tolerating D2 agonist monotherapy for longer periods, have slowly progressing forms of the disease. This may explain why randomly chosen patients treated with D2 agonists are more likely to drop-out clinical trials than those receiving levodopa (Holloway et al., 2004). Similarly, the highly debated issue of a neuroprotective effect of D2 agonists in clinical imaging studies is also suspected to result from drop-outs of patients with aggressive forms of the disease in settings receiving D2 agonist monotherapy (Parkinson Study Group, 2002). Accordingly, in one of the replicas used for the microarray experiments the pramipexole-treated rats had a significantly higher number of remaining dopaminergic neurons in the substantia nigra than levodopa-treated rats despite showing similar forelimb movement scores to those receiving levodopa (Fig. 4). Thus, our behavioral and histological studies: i. strengthen the predictive validity of the partial 6-OHDA lesion model (Kirik et al., 1998); ii. provide experimental support to the view that the therapeutic benefit obtained from D2 agonists depends on the degree of nigrostriatal degeneration; iii. indicate that the observed gene expression patterns correspond to clinically relevant therapeutic regimes.

The main finding of our genome-wide transcript expression analysis was that each drug treatment induced a singular gene expression pattern, involving relatively small but significant changes in a large number of transcripts. A direct comparison between levodopa-treated and pramipexole-treated rats yielded more than 500 differing transcripts. The changes in transcript expression found in the microarray assay were validated with a sample of 21 comparisons by qRT-PCR analysis. Overall, the fold changes observed with one technique were linearly related to those measured with the other one, except for two of the comparisons that gave diametrically opposite results. Differences in the assessment of transcription by the two methods could be due to the different gene sequences targeted by the probes used by each technique, but it may also reflect technical limitations in assessing small quantitative variations in gene expression with both methods. Although these drawbacks stress the need of validating each transcript of interest before drawing definitive conclusions, hierarchical clustering has correctly segregated both drug-induced gene expression patterns from the vehicle pattern, and also the drug-induced patterns from each other, strongly supporting that different gene expression patterns lie behind levodopa and pramipexole therapies.

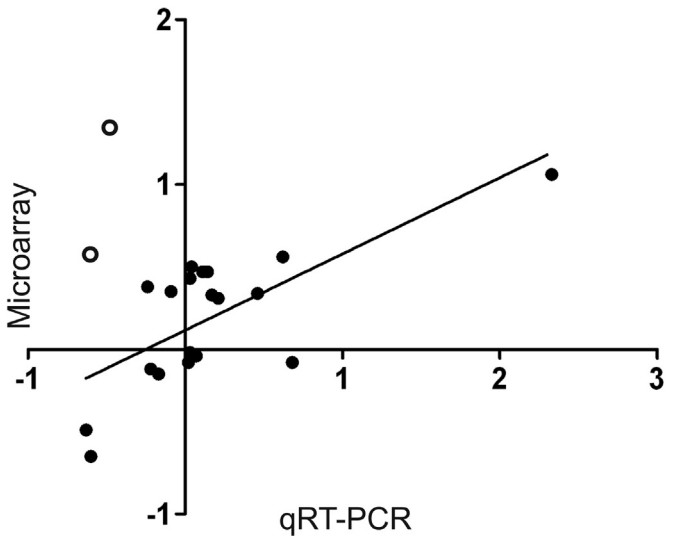

Fig. 6. Fold change values of microarray *versus* quantitative real-time RT-PCR (qRT-PCR). Correlated fold changes levels of expression for the selected genes indicated in Table 3. Microarray expression data from each gene was plotted against its qRT-PCR fold change and subjected to Pearson correlation analysis. Each point represents a single gene. The open circles were not included in the linear regression ($r = 0.72$, slope $= 0.46$, $p < 0.0006$).

Because of the overall small modifications in gene expression levels, we looked at coordinated changes involving families of functionally-related transcripts rather than at differences in the fold change of isolated transcripts. Studies using the KEGG database revealed an enrichment of transcripts from molecular pathways related to oxidative metabolism, mitochondrial function and oxidative stress in animals treated with levodopa relative to vehicle-treated and pramipexole-treated animals (Table 2). Although there are many possible scenarios for the origin of these changes, increased expression of electron transport complex proteins and mitochondrial membrane carriers may be an adaptation to the higher metabolic demands imposed by levodopa to functionally altered striatal circuits. In turn, increased oxidative metabolism may give rise to higher basal levels of oxidative stress in mitochondria (Surmeier and Schumacker, 2013), which may induce adaptations in the expression of transcripts regulating oxidative stress like superoxide dismutase 1 (SOD1) and glutathione peroxidase (GPx) (Ferrario et al., 2004).

Interestingly, some of the transcripts modified by levodopa within the oxidative metabolism KEGG pathway have also been related to apoptosis-related processes in mitochondria. Thus, SLC25a4 codes for a carrier that translocates ADP for ATP through the mitochondrion's inner membrane but also takes part of the permeability transition pore during apoptosis (Clémençon et al., 2013), and the serine peptidase HTRA2 normally protects mitochondrial DNA from oxidative stress but also contributes to triggering degeneration when released through the permeability transition pore (Plun-Favreau et al., 2007). That levodopa increases oxidative stress in the brain has been repeatedly reported and linked to presumptive toxic effects accelerating disease progression (Melamed et al., 1998; Müller and Muhlack, 2011; Ziv et al., 1997). Studies of the nigrostriatal system in animal models of the disease (Dziewczapolski et al., 1997b; Ferrario et al., 2004; Murer et al., 1998) and imaging studies in patients (Fahn, 2006, 2005) dispelled the fear that levodopa could accelerate nigrostriatal degeneration. Though, it has been repeatedly reported in patients and animals models that chronic levodopa induces a contraction of the dendritic arbors and reduces spine number in striatal “medium spiny” principal neurons (Day et al., 2006; Ingham et al., 1998, 1989; McNeill et al., 1988; Suárez et al., 2014; Zaja-Milatovic et al., 2005). In this regard it is tempting to speculate that basal increased levels of oxidative stress resulting from increased metabolic demands and/or directly induced by the levodopa treatment put striatal neurons at risk of losing dendritic surface and spines, which in the long term may reduce the therapeutic benefit obtained with levodopa and favor the appearance of motor complications.

An unexpected finding was the enrichment of transcripts encoding for olfactory receptor proteins in both levodopa and pramipexole-treated animals. Olfactory receptor proteins constitute a large family of 7-transmembrane domain G protein-coupled receptors mainly expressed in olfactory receptor cells, where they mediate transduction of odorant signals (Malnic et al., 2010). To our knowledge there are no previous reports about their expression or possible function in the striatum. Although “ectopic” expression of olfactory receptor proteins has been reported in several tissues (Flegel et al., 2013), whether this ectopic expression has a functional role has only been addressed in a few cases such as the testis and skeletal muscle (Griffin et al., 2009; Spehr et al., 2006). Alternatively, ectopic expression might not be associated with a specific function, but could be a byproduct of leaky

Please cite this article in press as: Taravini, I.R., et al., Contrasting gene expression patterns induced by levodopa and pramipexole treatments in the rat model of Parkinson's disease, Neuropharmacology (2015), http://dx.doi.org/10.1016/j.neuropharm.2015.04.018

transcriptional regulation mechanisms (Rodríguez-Trelles et al., 2005). Transcriptional regulation leakiness may be related to chromatin de-condensation required for the regulated expression of genes, which results in the exposure of additional regions of the genome to a limited repertoire of transcription factors. While transcriptional regulation leakiness may provide an evolutionary opportunity for protein diversification (Rodríguez-Trelles et al., 2005), it is worth asking whether transcriptional leakiness resulting from brain lesions or pharmacological treatments can be harmful in cells where the transduction machinery for olfactory receptor proteins is available. For instance, olfactory receptor proteins are over-expressed in some tumor cells where ligands for these receptors promote tissue invasion and metastasis emergence (Sanz et al., 2014). In this sense, G-alpha-olf, a G-protein co-expressed with olfactory receptor proteins in the olfactory receptor cells, is the main G-alpha subunit mediating D1 receptor signaling in the striatum (Zhuang et al., 2000). Overall, the data obtained here indicates the need for further understanding of the consequences of altered transcriptional regulation of olfactory transduction pathways in antiparkinsonian pharmacotherapy.

Acknowledgments

This work was supported by grants from Agencia Nacional para la Promoción de la Ciencia y la Tecnología (PICT 2011-1758; PICT 2013-1523), Universidad de Buenos Aires (UBACYT 2011-2014 20020100101004). GG and CF are research fellows of the Consejo Nacional de Investigaciones Científicas y Técnicas (CONICET). IT, EF and MGM are researchers from CONICET, Argentina.

Appendix A. Supplementary data

Supplementary data related to this article can be found at http://dx.doi.org/10.1016/j.neuropharm.2015.04.018.

References

Bennett, J.P., Piercey, M.F., 1999. Pramipexole—a new dopamine agonist for the treatment of Parkinson's disease. J. Neurol. Sci. 163, 25–31.

Carvalho, B., Bengtsson, H., Speed, T.P., Irizarry, R.A., 2007. Exploration, normalization, and genotype calls of high-density oligonucleotide SNP array data. Biostatistics 8, 485–499. http://dx.doi.org/10.1093/biostatistics/kxl042.

Carvalho, B.S., Irizarry, R.A., 2010. A framework for oligonucleotide microarray preprocessing. Bioinformatics 26, 2363–2367. http://dx.doi.org/10.1093/bioinformatics/btq431.

Cenci, M.A., Konradi, C., 2010. Maladaptive striatal plasticity in L-DOPA-induced dyskinesia. Prog. Brain Res. 183, 209–233. http://dx.doi.org/10.1016/S0079-6123(10)83011-0.

Cenci, M.A., Lundblad, M., 2007. Ratings of L-DOPA-induced dyskinesia in the unilateral 6-OHDA lesion model of Parkinson's disease in rats and mice. Curr. Protoc. Neurosci. http://dx.doi.org/10.1002/0471142301.ns0925s41. Chapter 9, Unit 9.25.

Clémençon, B., Babot, M., Trézéguet, V., 2013. The mitochondrial ADP/ATP carrier (SLC25 family): pathological implications of its dysfunction. Mol. Asp. Med. 34, 485–493. http://dx.doi.org/10.1016/j.mam.2012.05.006.

Cotzias, G.C., Papavasiliou, P.S., Gellene, R., 1969. Modification of Parkinsonism—chronic treatment with L-dopa. N. Engl. J. Med. 280, 337–345. http://dx.doi.org/10.1056/NEJM196902132800701.

Datla, K.P., Blunt, S.B., Dexter, D.T., 2001. Chronic L-DOPA administration is not toxic to the remaining dopaminergic nigrostriatal neurons, but instead may promote their functional recovery, in rats with partial 6-OHDA or FeCl(3) nigrostriatal lesions. Mov. Disord. 16, 424–434.

Day, M., Wang, Z., Ding, J., An, X., Ingham, C.A., Shering, A.F., Wokosin, D., Ilijic, E., Sun, Z., Sampson, A.R., Mugnaini, E., Deutch, A.Y., Sesack, S.R., Arbuthnott, G.W., Surmeier, D.J., 2006. Selective elimination of glutamatergic synapses on striatopallidal neurons in Parkinson disease models. Nat. Neurosci. 9, 251–259. http://dx.doi.org/10.1038/nn1632.

Delfino, M.A., Stefano, A.V., Ferrario, J.E., Taravini, I.R.E., Murer, M.G., Gershanik, O.S., 2004. Behavioral sensitization to different dopamine agonists in a parkinsonian rodent model of drug-induced dyskinesias. Behav. Brain Res. 152, 297–306. http://dx.doi.org/10.1016/j.bbr.2003.10.009.

Dziewczapolski, G., Mora, M.A., Menalled, L.B., Stéfano, F.J., Rubinstein, M., Gershanik, O.S., 1997a. Threshold of dopamine content and D1 receptor stimulation necessary for the expression of rotational behavior induced by D2 receptor stimulation under normo and supersensitive conditions. Naunyn Schmiedeb. Arch. Pharmacol. 355, 30–35.

Dziewczapolski, G., Murer, G., Agid, Y., Gershanik, O., Raisman-Vozari, R., 1997b. Absence of neurotoxicity of chronic L-DOPA in 6-hydroxydopamine-lesioned rats. Neuroreport 8, 975–979.

Fahn, S., 2006. A new look at levodopa based on the ELLDOPA study. J. Neural Transm. Suppl. 419–426.

Fahn, S., 2005. Does levodopa slow or hasten the rate of progression of Parkinson's disease? J. Neurol. 252 (Suppl. l), IV37–IV42. http://dx.doi.org/10.1007/s00415-005-4008-5.

Ferrario, J.E., Taravini, I.R.E., Mourlevat, S., Stefano, A., Delfino, M.A., Raisman-Vozari, R., Murer, M.G., Ruberg, M., Gershanik, O., 2004. Differential gene expression induced by chronic levodopa treatment in the striatum of rats with lesions of the nigrostriatal system. J. Neurochem. 90, 1348–1358. http://dx.doi.org/10.1111/j.1471-4159.2004.02595.x.

Flegel, C., Manteniotis, S., Osthold, S., Hatt, H., Gisselmann, G., 2013. Expression profile of ectopic olfactory receptors determined by deep sequencing. PLoS One 8, e55368. http://dx.doi.org/10.1371/journal.pone.0055368.

Griffin, C.A., Kafadar, K.A., Pavlath, G.K., 2009. MOR23 promotes muscle regeneration and regulates cell adhesion and migration. Dev. Cell. 17, 649–661. http://dx.doi.org/10.1016/j.devcel.2009.09.004.

Grünblatt, E., Schmidt, W.J., Scheller, D.K.A., Riederer, P., Gerlach, M., 2011. Transcriptional alterations under continuous or pulsatile dopaminergic treatment in dyskinetic rats. J. Neural Transm. 118, 1717–1725. http://dx.doi.org/10.1007/s00702-010-0552-y.

Holloway, R.G., Shoulson, I., Fahn, S., Kieburtz, K., Lang, A., Marek, K., McDermott, M., Seibyl, J., Weiner, W., Musch, B., Kamp, C., Welsh, M., Shinaman, A., Pahwa, R., Barclay, L., Hubble, J., LeWitt, P., Miyasaki, J., Suchowersky, O., Stacy, M., Russell, D.S., Ford, B., Hammerstad, J., Riley, D., Standaert, D., Wooten, F., Factor, S., Jankovic, J., Atassi, F., Kurlan, R., Panisset, M., Rajput, A., Rodnitzky, R., Shults, C., Petsinger, G., Waters, C., Pfeiffer, R., Biglan, K., Borchert, L., Montgomery, A., Sutherland, L., Weeks, C., DeAngelis, M., Sime, E., Wood, S., Pantella, C., Harrigan, M., Fussell, B., Dillon, S., Alexander-Brown, B., Rainey, P., Tennis, M., Rost-Ruffner, E., Brown, D., Evans, S., Berry, D., Hall, J., Shirley, T., Dobson, J., Fontaine, D., Pfeiffer, B., Brocht, A., Bennett, S., Daigneault, S., Hodgeman, K., O'Connell, C., Ross, T., Richard, K., Watts, A., 2004. Pramipexole vs levodopa as initial treatment for Parkinson disease: a 4-year randomized controlled trial. Arch. Neurol. 61, 1044–1053. http://dx.doi.org/10.1001/archneur.61.7.1044.

Ingham, C.A., Hood, S.H., Arbuthnott, G.W., 1989. Spine density on neostriatal neurones changes with 6-hydroxydopamine lesions and with age. Brain Res. 503, 334–338.

Ingham, C.A., Hood, S.H., Taggart, P., Arbuthnott, G.W., 1998. Plasticity of synapses in the rat neostriatum after unilateral lesion of the nigrostriatal dopaminergic pathway. J. Neurosci. 18, 4732–4743.

Jenner, P., 2008. Molecular mechanisms of L-DOPA-induced dyskinesia. Nat. Rev. Neurosci. 9, 665–677. http://dx.doi.org/10.1038/nrn2471.

Kirik, D., Rosenblad, C., Björklund, a, 1998. Characterization of behavioral and neurodegenerative changes following partial lesions of the nigrostriatal dopamine system induced by intrastriatal 6-hydroxydopamine in the rat. Exp. Neurol. 152, 259–277. http://dx.doi.org/10.1006/exnr.1998.6848.

Konradi, C., Westin, J.E., Carta, M., Eaton, M.E., Kuter, K., Dekundy, A., Lundblad, M., Cenci, M.A., 2004. Transcriptome analysis in a rat model of L-DOPA-induced dyskinesia. Neurobiol. Dis. 17, 219–236. http://dx.doi.org/10.1016/j.nbd.2004.07.005.

Larramendy, C., Taravini, I.R.E., Saborido, M.D., Ferrario, J.E., Murer, M.G., Gershanik, O.S., 2008. Cabergoline and pramipexole fail to modify already established dyskinesias in an animal model of parkinsonism. Behav. Brain Res. 194, 44–51. http://dx.doi.org/10.1016/j.bbr.2008.06.021.

Livak, K.J., Schmittgen, T.D., 2001. Analysis of relative gene expression data using real-time quantitative PCR and the 2(-Delta Delta C(T)) Method. Methods 25, 402–408. http://dx.doi.org/10.1006/meth.2001.1262.

Lundblad, M., Picconi, B., Lindgren, H., Cenci, M.A., 2004. A model of L-DOPA-induced dyskinesia in 6-hydroxydopamine lesioned mice: relation to motor and cellular parameters of nigrostriatal function. Neurobiol. Dis. 16, 110–123. http://dx.doi.org/10.1016/j.nbd.2004.01.007.

Malnic, B., Gonzalez-Kristeller, D.C., Gutiyama, L.M., 2010. Odorant receptors [The neurobiology of olfaction. 2010]. PubMed – NCBI. In: Menini, A. (Ed.), Frontiers in Neuroscience. CRC Press, Boca Raton (FL).

Marie-Claire, C., Courtin, C., Roques, B.P., Noble, F., 2004. Cytoskeletal genes regulation by chronic morphine treatment in rat striatum. Neuropsychopharmacology 29, 2208–2215.

Marin, C., Bonastre, M., Mengod, G., Cortés, R., Giralt, A., Obeso, J.A., Schapira, A.H., 2014. Early L-dopa, but not pramipexole, restores basal ganglia activity in partially 6-OHDA-lesioned rats. Neurobiol. Dis. 64, 36–47. http://dx.doi.org/10.1016/j.nbd.2013.12.009.

McCarthy, D.J., Smyth, G.K., 2009. Testing significance relative to a fold-change threshold is a TREAT. Bioinformatics 25, 765–771. http://dx.doi.org/10.1093/bioinformatics/btp053.

McNeill, T.H., Brown, S.A., Rafols, J.A., Shoulson, I., 1988. Atrophy of medium spiny I striatal dendrites in advanced Parkinson's disease. Brain Res. 455, 148–152.

Melamed, E., Offen, D., Shirvan, A., Djaldetti, R., Barzilai, A., Ziv, I., 1998. Levodopa toxicity and apoptosis. Ann. Neurol. 44, S149–S154.

Please cite this article in press as: Taravini, I.R., et al., Contrasting gene expression patterns induced by levodopa and pramipexole treatments in the rat model of Parkinson's disease, Neuropharmacology (2015), http://dx.doi.org/10.1016/j.neuropharm.2015.04.018

Meurers, B.H., Dziewczapolski, G., Shi, T., Bittner, A., Kamme, F., Shults, C.W., 2009. Dopamine depletion induces distinct compensatory gene expression changes in DARPP-32 signal transduction cascades of striatonigral and striatopallidal neurons. J. Neurosci. 29, 6828–6839. http://dx.doi.org/10.1523/JNEUROSCI.5310-08.2009.

Müller, T., Muhlack, S., 2011. Cysteinyl-glycine reduction as marker for levodopa-induced oxidative stress in Parkinson's disease patients. Mov. Disord. 26, 543–546. http://dx.doi.org/10.1002/mds.23384.

Murer, M.G., Dziewczapolski, G., Menalled, L.B., García, M.C., Agid, Y., Gershanik, O., Raisman-Vozari, R., 1998. Chronic levodopa is not toxic for remaining dopamine neurons, but instead promotes their recovery, in rats with moderate nigrostriatal lesions. Ann. Neurol. 43, 561–575. http://dx.doi.org/10.1002/ana.410430504.

Murer, M.G., Moratalla, R., 2011. Striatal signaling in L-DOPA-induced dyskinesia: common mechanisms with drug abuse and long term memory involving D1 dopamine receptor stimulation. Front. Neuroanat. 5, 51. http://dx.doi.org/10.3389/fnana.2011.00051.

Murer, M.G., Raisman-Vozari, R., Gershanik, O., 1999. Levodopa in Parkinson's disease: neurotoxicity issue laid to rest? Drug Saf. 21, 339–352.

Olanow, C.W., Agid, Y., Mizuno, Y., Albanese, A., Bonuccelli, U., Bonucelli, U., Damier, P., De Yebenes, J., Gershanik, O., Guttman, M., Grandas, F., Hallett, M., Hornykiewicz, O., Jenner, P., Katzenschlager, R., Langston, W.J., LeWitt, P., Melamed, E., Mena, M.A., Michel, P.P., Mytilineou, C., Obeso, J.A., Poewe, W., Quinn, N., Raisman-Vozari, R., Rajput, A.H., Rascol, O., Sampaio, C., Stocchi, F., 2004. Levodopa in the treatment of Parkinson's disease: current controversies. Mov. Disord. 19, 997–1005. http://dx.doi.org/10.1002/mds.20243.

Olsson, M., Nikkhah, G., Bentlage, C., Björklund, A., 1995. Forelimb akinesia in the rat Parkinson model: differential effects of dopamine agonists and nigral transplants as assessed by a new stepping test. J. Neurosci. 15, 3863–3875.

Parkinson Study Group, 2009. Long-term effect of initiating pramipexole vs levodopa in early Parkinson disease. Arch. Neurol. 66, 563–570. http://dx.doi.org/10.1001/archneur.66.1.nct90001.

Parkinson Study Group, 2002. Dopamine transporter brain imaging to assess the effects of pramipexole vs levodopa on Parkinson disease progression. JAMA 287, 1653–1661.

Parkinson Study Group, 2000. Pramipexole vs levodopa as initial treatment for Parkinson disease: a randomized controlled trial. Parkinson Study Group JAMA 284, 1931–1938.

Paxinos, G., Watson, C., 1986. The Rat Brain in Stereotaxic Coordinates. Academic Press Inc., San Diego.

Pd Med Collaborative Group, 2014. Long-term effectiveness of dopamine agonists and monoamine oxidase B inhibitors compared with levodopa as initial treatment for Parkinson's disease (PD MED): a large, open-label, pragmatic randomised trial. Lancet. http://dx.doi.org/10.1016/S0140-6736(14)60683-8.

Plun-Favreau, H., Klupsch, K., Moisoi, N., Gandhi, S., Kjaer, S., Frith, D., Harvey, K., Deas, E., Harvey, R.J., McDonald, N., Wood, N.W., Martins, L.M., Downward, J., 2007. The mitochondrial protease HtrA2 is regulated by Parkinson's disease-associated kinase PINK1. Nat. Cell. Biol. 9, 1243–1252. http://dx.doi.org/10.1038/ncb1644.

Robertson, G.S., Robertson, H.A., 1986. Synergistic effects of D1 and D2 dopamine agonists on turning behaviour in rats. Brain Res. 384, 387–390.

Rodríguez-Trelles, F., Tarrío, R., Ayala, F.J., 2005. Is ectopic expression caused by deregulatory mutations or due to gene-regulation leaks with evolutionary potential? Bioessays 27, 592–601. http://dx.doi.org/10.1002/bies.20241.

Sanz, G., Leray, I., Dewaele, A., Sobilo, J., Lerondel, S., Bouet, S., Grébert, D., Monnerie, R., Pajot-Augy, E., Mir, L.M., 2014. Promotion of cancer cell invasiveness and metastasis emergence caused by olfactory receptor stimulation. PLoS One 9, e85110. http://dx.doi.org/10.1371/journal.pone.0085110.

Schallert, T., Fleming, S.M., Leasure, J.L., Tillerson, J.L., Bland, S.T., 2000. CNS plasticity and assessment of forelimb sensorimotor outcome in unilateral rat models of stroke, cortical ablation, parkinsonism and spinal cord injury. Neuropharmacology 39, 777–787.

Schapira, A.H.V., McDermott, M.P., Barone, P., Comella, C.L., Albrecht, S., Hsu, H.H., Massey, D.H., Mizuno, Y., Poewe, W., Rascol, O., Marek, K., 2013. Pramipexole in patients with early Parkinson's disease (PROUD): a randomised delayed-start trial. Lancet Neurol. 12, 747–755. http://dx.doi.org/10.1016/S1474-4422(13)70117-0.

Smyth, G., 2005. Limma: linear models for microarray data. In: Gentleman, Robert, Carey, Vincent J., Huber, Wolfgang, Irizarry, Rafael A., Dudoit, S. (Eds.), Bioinformatics and Computational Biology Solutions Using R and Bioconductor. Springer New York, New York, pp. 397–420. http://dx.doi.org/10.1007/0-387-29362-0_23.

Spehr, M., Schwane, K., Riffell, J.A., Zimmer, R.K., Hatt, H., 2006. Odorant receptors and olfactory-like signaling mechanisms in mammalian sperm. Mol. Cell. Endocrinol. 250, 128–136. http://dx.doi.org/10.1016/j.mce.2005.12.035.

Suárez, L.M., Solís, O., Caramés, J.M., Taravini, I.R., Solís, J.M., Murer, M.G., Moratalla, R., 2014. L-DOPA treatment selectively restores spine density in dopamine receptor D2-expressing projection neurons in dyskinetic mice. Biol. Psychiatry 75, 711–722. http://dx.doi.org/10.1016/j.biopsych.2013.05.006.

Surmeier, D.J., Schumacker, P.T., 2013. Calcium, bioenergetics, and neuronal vulnerability in Parkinson's disease. J. Biol. Chem. 288, 10736–10741. http://dx.doi.org/10.1074/jbc.R112.410530.

Taravini, I.R., Chertoff, M., Cafferata, E.G., Courty, J., Murer, M.G., Pitossi, F.J., Gershanik, O.S., 2011. Pleiotrophin over-expression provides trophic support to dopaminergic neurons in parkinsonian rats. Mol. Neurodegener. 6, 40. http://dx.doi.org/10.1186/1750-1326-6-40.

Treseder, S.A., Smith, L.A., Jenner, P., 2000. Endogenous dopaminergic tone and dopamine agonist action. Mov. Disord. 15, 804–812.

Werner, T., 2008. Bioinformatics applications for pathway analysis of microarray data. Curr. Opin. Biotechnol. 19, 50–54. http://dx.doi.org/10.1016/j.copbio.2007.11.005.

Wilkinson, L., Friendly, M., 2009. The history of the cluster heat map. Am. Stat. 63, 179–184. http://dx.doi.org/10.1198/tas.2009.0033.

Woodlee, M.T., Asseo-García, A.M., Zhao, X., Liu, S.-J., Jones, T.A., Schallert, T., 2005. Testing forelimb placing "across the midline" reveals distinct, lesion-dependent patterns of recovery in rats. Exp. Neurol. 191, 310–317. http://dx.doi.org/10.1016/j.expneurol.2004.09.005.

Zaja-Milatovic, S., Milatovic, D., Schantz, A.M., Zhang, J., Montine, K.S., Samii, A., Deutch, A.Y., Montine, T.J., 2005. Dendritic degeneration in neostriatal medium spiny neurons in Parkinson disease. Neurology 64, 545–547. http://dx.doi.org/10.1212/01.WNL.0000150591.33787.A4.

Zhuang, X., Belluscio, L., Hen, R., 2000. G(olf)alpha mediates dopamine D1 receptor signaling. J. Neurosci. 20, RC91.

Ziv, I., Zilkha-Falb, R., Offen, D., Shirvan, A., Barzilai, A., Melamed, E., 1997. Levodopa induces apoptosis in cultured neuronal cells–a possible accelerator of nigrostriatal degeneration in Parkinson's disease? Mov. Disord. 12, 17–23. http://dx.doi.org/10.1002/mds.870120105.

Please cite this article in press as: Taravini, I.R., et al., Contrasting gene expression patterns induced by levodopa and pramipexole treatments in the rat model of Parkinson's disease, Neuropharmacology (2015), http://dx.doi.org/10.1016/j.neuropharm.2015.04.018